Thermochimica Acta, 162 (1990) 229–240
Elsevier Science Publishers B.V., Amsterdam – Printed in The Netherlands

CRYSTAL STRUCTURE AND THERMODYNAMICS OF PHASE TRANSITIONS OF *N*-ACETYL-L-VALINAMIDE *

R. PULITI

Istituto per la Chimica di Molecole di Interesse Biologico del C.N.R., via Toiano 6, 80072 Arco-Felice, Napoli (Italy)

C.A. MATTIA and G. BARONE

Dipartimento di Chimica, Università "Federico II" di Napoli, via Mezzocannone 4, 80134 Napoli (Italy)

G. DELLA GATTA

Dipartimento di Chimica Inorganica, Chimica Fisica e Chimica dei Materiali, Università di Torino, via P. Giuria 9, 10125 Torino (Italy)

D. FERRO

Centro per la Termodinamica Chimica alle Alte Temperature del C.N.R., Dipartimento di Chimica, Università "La Sapienza" di Roma, P. le A. Moro 5, 00185 Roma (Italy)

(Received in final form 14 September 1989)

ABSTRACT

Changes in the fundamental thermodynamic functions, such as enthalpy and entropy, during fusion and sublimation have been measured for *N*-acetyl-L-valinamide (L-NAVA) and compared with previous results for the same derivative of other simple amino acids (glycine, L-alanine and D-leucine).

There is no discernible simple relation between the increasing molecular weight and any of the measured quantities. The fusion properties of L-NAVA are characterised by values noticeably higher than those of other homologous compounds, the sublimation properties being intermediate between those of the glycine and alanine derivatives.

An accurate crystallographic analysis of L-NAVA has been carried out to support this observed behaviour. Detailed knowledge of the molecular orientations and contacts in the crystal is required because L-NAVA has the same number of H-bonds as the derivatives of glycine and alanine, although its density is very close to that of the leucine derivative, whose packing is characterised by a lower number of H-bonds.

In order to optimise the intermolecular interactions and to adhere to the conformational constraints, the L-NAVA molecules are arranged in the crystal such that the hydrogen bonds are of proper length and there are good van der Waals contacts between some of the alkyl

* Presented at the 10th AICAT, Pisa, Italy, 11–14 December 1988.

0040-6031/90/$03.50

groups. The relatively high stability of L-NAVA crystals can be attributed to these factors. At the same time there are regions of small voids, which are responsible for the relatively low density.

INTRODUCTION

As part of a programme on the study of the solid state properties of molecules which act as models of biological macromolecules, we have recently investigated both the phase transition thermodynamics [1,2] and the crystal structures [3,4] of an interesting class of uncharged molecules: the amides of *N*-acetyl amino acids. These substances have been shown to be useful models for peptide interactions in solution [5–9]. In this regard, reliable data for the sublimation enthalpies of solid organic compounds are of great interest, in particular because they can be combined with the enthalpies of solution at infinite dilution in water or in organic solvents to obtain the relevant solvation enthalpies and provide an insight into the solute–solvent interactions. Furthermore, a scan between the experimental temperatures of solution, usually close to 298 K, and those of sublimation, is indispensable for the detection of possible solid-to-solid transitions. These transition enthalpies, if found, must be taken into account in the derivation of solvation parameters.

One of these amino acid derivatives, *N*-acetyl-L-valinamide (L-NAVA), has attracted our attention because of its exceptionally high fusion temperature (509 K compared with 404–431 K for other amides). For this reason, in addition to the enthalpy and entropy of sublimation, we have also determined the enthalpy and entropy of fusion. In the first paper of this series [1], it was shown that the sublimation and fusion enthalpies decrease from the amide of *N*-acetylglycine (NAGA) to that of *N*-acetyl-L-alanine (L-NAAA) and *N*-acetyl-D-leucine (D-NALA), on increasing the molecular weight. This unusual trend was correlated with the crystal structures of these substances [3].

As will be seen, L-NAVA shows intermediate crystal properties because the number of hydrogen bonds shared by each molecule is six, as for NAGA and L-NAAA, whereas the density (1.135 g cm^{-3}) is very close to that of D-NALA. In contrast, the temperature, and enthalpy and entropy of fusion of L-NAVA are higher than those of NAGA and L-NAAA (and also D-NALA), the enthalpy and entropy of sublimation being intermediate between those of NAGA and those of L-NAAA and D-NALA (which are lower).

In this paper, the X-ray analysis is presented in detail to provide at least a qualitative explanation of the relatively greater stability of the L-NAVA crystals.

EXPERIMENTAL

Materials

The *N*-acetyl-L-valinamide was synthetised according to Blackburn et al. [5]. The product was purified by several crystallisations and dried under vacuum. Repeated checks, by thin layer chromatography and polarimetry, were performed to ascertain the purity and the absence of racemisation in the final product.

High purity indium (5N8, Koch-Light) and naphthalene (reference material, purity grade, Farmitalia-Carlo Erba) were used as standards for calorimetric and vapour pressure measurements, respectively.

Vapour pressure measurements

Vapour pressures were measured by the torsion–effusion technique [10,11], as already described in detail [1,12–14]. In this study, two conventional graphite cells were used with a total of four runs. Temperatures were measured with a calibrated chromel–alumel thermocouple with a precision of ± 0.5 K. The temperature range explored was 391–445 K, because the vapour pressures cannot be measured at lower temperatures with small errors. The range is large enough to limit the uncertainty in the enthalpy values.

Calorimetric measurements

The enthalpy and temperature of fusion were measured with a Setaram DSC-111G differential scanning apparatus. An aluminium and a stainless steel cell were used. The experimental details and the procedure used to calculate the heat values have been described elsewhere [15]. All fusion runs were performed at a heating rate of 1 K min^{-1}. No solid-to-solid transitions were observed from room temperature to the melting point.

Crystal data and structure determination

Single crystals of L-NAVA were obtained, by careful recrystallisation from methanol, in the form of small colourless prisms elongated along the *b* axis. A crystal of approximate size $0.50 \times 0.11 \times 0.04$ mm was selected for the crystallographic study. Accurate cell parameters were obtained by least-squares refinement of the setting angles of 24 reflections at medium θ ($21° \leq \theta \leq 27°$), using monochromated Cu $K\alpha$ radiation and an Enraf–Nonius CAD-4F diffractometer on line with a MicroVAX computer. Crystal data were as follows: formula $C_7H_{14}N_2O_2$; $M_w = 158.2$; monoclinic system; space group $C2$, with $Z = 2$, $a = 13.493(2)$ Å, $b = 4.834(1)$ Å, $c = 14.230(2)$

Å, $\beta = 94.05(1)°$, $V = 925.9(8)$ Å^3 and $D_c = 1.135$ g cm^{-3}. 985 independent reflections ($\theta_{max} = 70°$) were collected at room temperature, using ω scan mode, as suggested by peak-shape analysis. During the data collection, the intensities of three standard reflections were monitored every 4 h (4% max. variation) in order to check the crystal and equipment stability. The intensities were corrected for Lorentz and polarisation factors, but not for the absorption effect (μ(Cu $K\alpha$) = 0.65 mm^{-1}). The structure was solved by direct methods using the MULTAN 82 program [16]. The refinement of positional and anisotropic temperature parameters for non-hydrogen atoms was carried out by full-matrix (on F) least-squares method. All hydrogens were unambiguously located from a difference electron-density map and included in the last refinement cycles with isotropic thermal parameters fixed equal to the B_{eq} of the parent atoms (only positional parameters were refined for H-atoms). At convergence the final discrepancy index, $R = \Sigma || F_0 | - | F_c || / \Sigma | F_0 |$, was 0.038 * for the 873 observed reflections with $I > 2.5\ \sigma(I)$ and 142 variables, including a correction for secondary extinction: g coefficient = $1.7(1) \times 10^{-5}$, $R_w = 0.041$ with $w = 1/[\sigma F^2 + (0.02F)^2 + 1]$ and σ from counting statistics.

Atomic scattering factors were taken from Cromer and Waber [17]. Enraf–Nonius SDP software (1985) and the MicroVAX computer of the Centro di Metodologie Chimico-fisiche dell'Università di Napoli were used for the crystallographic work.

RESULTS AND DISCUSSION

Thermodynamics

The dependence of the vapour pressure on temperature follows the classical equation

$$\log p = A - B/T = \Delta_{sub} S^{\ominus}_{T_{av}}/2.303R - \Delta_{sub} H^{\ominus}_{T_{av}}/2.303RT \quad (1)$$

where R is the gas constant and the sublimation enthalpy and entropy are derived, according to the second-law method, at T_{av} (the average value of the experimental temperature range). Equations from the least-squares treatment of the experimental data for each run are reported in Table 1. By weighting slopes and intercepts according to the number of experimental data, the following equation was selected

$$\log p = 14.00(0.30) - 6589(120)(1/T) \quad (2)$$

where p is in kPa and T is in K. The weighted standard deviations are given in parentheses.

* Supplementary material, containing a list of structure factors and anisotropic thermal parameters, is available on request.

TABLE 1

Vapour pressure against $1/T$ equations for *N*-acetyl-L-valinamide

Run (cell) [a]	Temperature range (K)	No. of points	$\log p = A - B/T$	
			A [b]	B [b] (*K*)
1 (A)	398–445	23	13.73(22)	6447(93)
2 (A)	394–443	14	14.19(34)	6665(145)
3 (B)	391–425	15	14.20(24)	6690(98)
4 (B)	395–417	12	14.10(42)	6645(173)

[a] Cell A, $\phi = 1.00(0.05)$ mm; cell B, $\phi = 1.20(0.05)$ mm.
[b] Figures in parentheses are the reported standard deviations.

The calculated sublimation enthalpy $\Delta_{sub}H^{\ominus}_{T_{av}} = 126(2)$ kJ mol^{-1} is intermediate between that of NAGA (135 kJ mol^{-1}) and those of L-NAAA and D-NALA (115 and 101 kJ mol^{-1} respectively) evaluated in comparable temperature ranges [1]. The entropy of sublimation for L-NAVA, $\Delta_{sub}S^{\ominus}_{T_{av}} =$ 230(6) J mol^{-1} K^{-1}, is related to those of other amides in the same manner as the enthalpy, the values being 256, 212 and 178 J mol^{-1} K^{-1} for NAGA, L-NAAA and D-NALA respectively [1].

Correlations between the thermodynamic sublimation parameters and molecular structure are not extensively established for organic compounds [18], but an increase with increasing molecular dimensions is usually expected, in particular when aliphatic chains are concerned [19]. Substantially constant contributions for each additional $-CH_2-$ group to the sublimation

TABLE 2

Measurements by DSC of temperatures and enthalpies of fusion of *N*-acetyl-L-valinamide [a]

m (g)	Crucible	T_{fus} (K)	*A* (mm^2)	*S* (μV mW^{-1})	$\Delta_{fus}H$ (kJ mol^{-1})
0.00242	Al	508.75	2100	7.923	41.80
0.00709	Al	509.39	5910	7.925	40.18
0.00393	Al	508.71	3390	7.923	41.59
0.00621	Al	509.15	5350	7.924	41.54
0.00666	s.s. [b]	509.12	5600	7.920	40.58
0.00358	s.s. [b]	508.97	3070	7.920	41.36
0.00633	s.s. [b]	508.97	5490	7.919	41.84
0.00560	s.s. [b]	508.97	4790	7.919	41.27
		509.0(0.4) [c]			41.3(0.6) [c]

[a] The first column gives the amount of the compound, the second the kind of crucible used and the third the onset temperature of the fusion peak. The fourth column reports the measured area of the peak, the fifth the sensitivity (*S*) of the heat-flux detector [15] and the sixth the fusion enthalpy.
[b] s.s., Stainless steel.
[c] The mean values of temperature and enthalpy of fusion are reported together with their standard deviations.

TABLE 3

Enthalpies and entropies of sublimation and fusion for amides of *N*-acetyl amino acids

Compound	T_{av} [a] (K)	$\Delta_{sub}H^{\ominus}_{T_{av}}$ (kJ mol^{-1})	$\Delta_{sub}S^{\ominus}_{T_{av}}$ (J mol^{-1} K^{-1})	T_{fus} (K)	$\Delta_{fus}H^{\ominus}_{T}$ (kJ mol^{-1})	$\Delta_{fus}S^{\ominus}_{T}$ (J mol^{-1} K^{-1})
NAGA [b]	393	135(3)	256(6)	408.2(0.3)	25.6(0.4)	62.7(1.0)
L-NAAA [b]	388	115(3)	212(5)	431.0(0.4)	21.7(0.2)	50.3(0.5)
L-NAVA	418	126(2)	230(6)	509.0(0.4)	41.3(0.6)	81.1(0.9)
D-NALA [b]	392	101(3)	178(9)	404.0(0.1)	20.2(0.3)	50.0(0.7)

[a] Mean temperature of vapour pressure measurements.
[b] Data from ref. 1.

or vaporization enthalpies and entropies have been reported for normal alcohols [20], mono- and dicarboxylic acids [21], esters [22] and primary normal amides [23]. The reverse trend in the values of the sublimation parameters of L-NAVA and L-NAAA and of NAGA and D-NALA, however, is well established and cannot be attributed to experimental errors. An exceptional trend was also found during the fusion experiments (Table 2). The calorimetric runs, in fact, yielded $\Delta_{fus}H^{\ominus} = 41.3(0.6)$ and $T_{fus} = 507.5(1.3)$ for L-NAVA, values that are much higher than those of other studied amides. The same occurs, in consequence, for the fusion entropy $\Delta_{fus}S^{\ominus} = 81.3$ (1.6). All the thermodynamic data concerning the change of state of these solid amino acid derivatives are reported for comparison in Table 3.

X-ray analysis

The final atomic parameters are reported in Table 4. The intramolecular geometry concerning non-hydrogen atoms is given in Table 5, the bond lengths involving H-atoms lying in the range 0.87–1.09 Å. The bond distances and bond angles, on average, compare well with the values generally found for similar compounds (see ref. 24 and references therein). In the crystal, the backbone conformation of L-NAVA (see torsion angles in Table 5), is very similar to that recently found for *N*-acetyl-L-alaninamide [3] and falls in the E region of the φ–ψ conformational map showing the energy minima for several amino acid residues [25]. The side-chain conformation (tg^-) is that most frequently found in the L-valine derivatives. The overall conformation agrees with the statistical [26] and theoretical [27] results showing the correlation between the β-branching side-chain and backbone conformations.

Except for the isopropyl group, all non-hydrogen atoms lie, within the estimated standard deviation (e.s.d.) values in the two planes containing the C1, C2, N2, O1 and C1, N1, C3, C4, O2 atoms respectively. The dihedral angle between these best planes is 60.8(1)°.

TABLE 4

Positional parameters and equivalent isotropic thermal parameters (Å^2) (e.s.d. in parentheses): $B_{eq} = 4/3\ \Sigma_i\Sigma_j\beta_{ij}a_ia_j$

	x	y	z	B_{eq}
O1	0.9470(1)	0 [a]	0.2098(2)	5.24(5)
O2	0.7031(1)	0.7200(5)	0.1395(2)	4.47(4)
N1	0.7637(1)	0.2912(5)	0.1668(2)	3.22(4)
N2	1.0079(2)	0.4291(6)	0.2024(2)	4.95(6)
C1	0.8377(2)	0.3718(6)	0.2416(2)	3.15(5)
C2	0.9369(2)	0.2516(6)	0.2162(2)	3.56(5)
C3	0.7028(2)	0.4697(6)	0.1207(2)	3.34(5)
C4	0.6324(2)	0.3506(8)	0.0446(2)	4.40(6)
C5	0.8099(2)	0.2691(9)	0.3383(2)	4.87(7)
C6	0.8923(3)	0.349(1)	0.4132(3)	8.2(1)
C7	0.7104(3)	0.385(1)	0.3625(3)	6.7(1)
HN1	0.757(2)	0.112(8)	0.153(2)	3.2
HN2	1.001(2)	0.616(9)	0.212(2)	5.0
H′N2	1.067(2)	0.364(9)	0.189(2)	5.0
HC1	0.842(2)	0.586(8)	0.237(2)	3.1
HC4	0.636(2)	0.140(9)	0.041(2)	4.4
H′C4	0.642(2)	0.437(9)	−0.007(2)	4.4
H″C4	0.566(2)	0.368(9)	0.061(2)	4.4
HC5	0.809(2)	0.053(9)	0.335(3)	4.9
HC6	0.899(3)	0.56(1)	0.418(3)	8.2
H′C6	0.873(3)	0.32(1)	0.470(3)	8.2
H″C6	0.957(3)	0.31(1)	0.400(3)	8.2
HC7	0.707(3)	0.57(1)	0.366(3)	6.7
H′C7	0.691(3)	0.31(1)	0.414(3)	6.7
H″C7	0.650(3)	0.31(1)	0.315(3)	6.7

[a] Fixed to define the origin.

The crystal packing is stabilised by three different intermolecular hydrogen bonds, which involve all the peptidic and amidic hydrogens. Figure 1 shows a layer of hydrogen bonds extended parallel to the a–b plane. Infinite piles of molecules translated along the b direction are interlinked by pairs of H-bonds, N1–H · · · O2 and N2–H · · · O1. Moreover, the molecules belonging to different piles are connected by a third H-bond between the amidic nitrogen N2 and the acetylic oxygen O2. The geometry of the hydrogen bonds is given in Table 6.

The hydrogen bonding layers separate, along the c direction, two hydrophobic regions which contain one of the valine side-chains at $c = 0.5$ alternating with one of the C4 methyl groups at $c = 0$ (Fig. 2). In these apolar regions, the shortet intermolecular methyl–methyl distances are C6 · · · $C6_{2-x,y,1-z}$ = 3.679(5)Å and C4 · · · $C4_{1-x,y,-z}$ = 3.707(4) Å where the subscripts are the symmetry codes of the second atom. These van der Waals contacts, between the same group referred by diad axis, lie in the a–c plane.

TABLE 5

Intramolecular geometry (e.s.d. in parentheses)

Bond lengths (Å)			
O1–C2	1.228(3)	C1–C2	1.526(4)
O2–C3	1.239(4)	C1–C5	1.534(4)
N1–C1	1.459(3)	C3–C4	1.503(4)
N1–C3	1.332(3)	C5–C6	1.534(5)
N2–C2	1.311(4)	C5–C7	1.517(5)
Bond angles (deg)			
C1–N1–C3	123.6(2)	O2–C3–N1	122.3(2)
N1–C1–C2	107.0(2)	O2–C3–C4	121.4(3)
N1–C1–C5	111.7(2)	N1–C3–C4	116.3(3)
C2–C1–C5	111.3(2)	C1–C5–C6	109.3(3)
O1–C2–N2	123.5(2)	C1–C5–C7	111.1(3)
O1–C2–C1	119.9(2)	C6–C5–C7	111.1(3)
N2–C2–C1	116.7(3)		
Torsion angles (deg)			
C3–N1–C1–C2	−127.9(2)	C5–C1–C2–O1	60.4(4)
C3–N1–C1–C5	110.1(3)	C5–C1–C2–N2	−119.5(3)
C1–N1–C3–O2	−1.7(4)	N1–C1–C5–C6	177.6(3)
C1–N1–C3–C4	179.0(2)	N1–C1–C5–C7	−59.5(4)
N1–C1–C2–O1	−61.9(3)	C2–C1–C5–C6	58.1(4)
N1–C1–C2–N2	118.2(3)	C2–C1–C5–C7	−179.0(3)

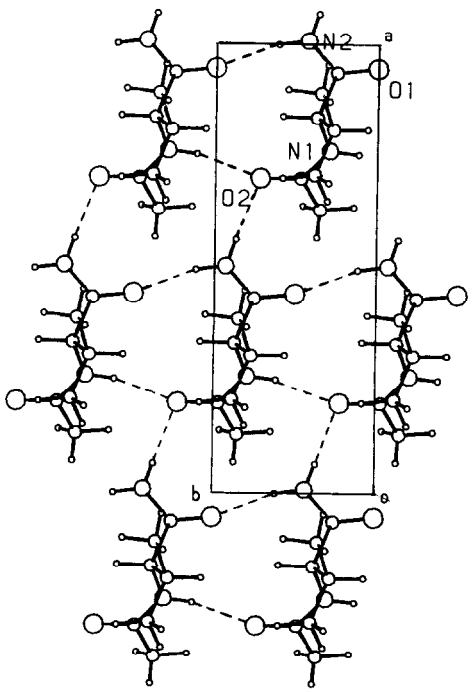

Fig. 1. Crystal packing of L-NAVA projected on the $a-b$ plane. Hydrogen bonds are indicated by dashed lines. For clarity, only the oxygen and nitrogen atoms are labelled.

TABLE 6

Hydrogen bonding geometry [a]

D–H···A	D···A (Å)	H···A (Å)	D–H···A (deg)	Symmetry of A
N1–HN1...O2	2.898(3)	2.04(4)	163(3)	$x, y-1, z$
N2–HN2...O1	2.884(3)	1.99(4)	162(3)	$x, y+1, z$
N2–H'N2...O2	3.015(3)	2.13(3)	173(3)	$x+1/2, y-1/2, z$

[a] D, Donor; A, acceptor.

In addition, in the regions containing the isopropyl side-chains, there are two other rather short van der Waals interactions, extending along the *b* axis: $C6 \cdots C7_{3/2-x,y-1/2,1-z} = 4.215(6)$Å and $C6 \cdots C7_{3/2-x,1/2+y,1-z} = 4.411(5)$Å.

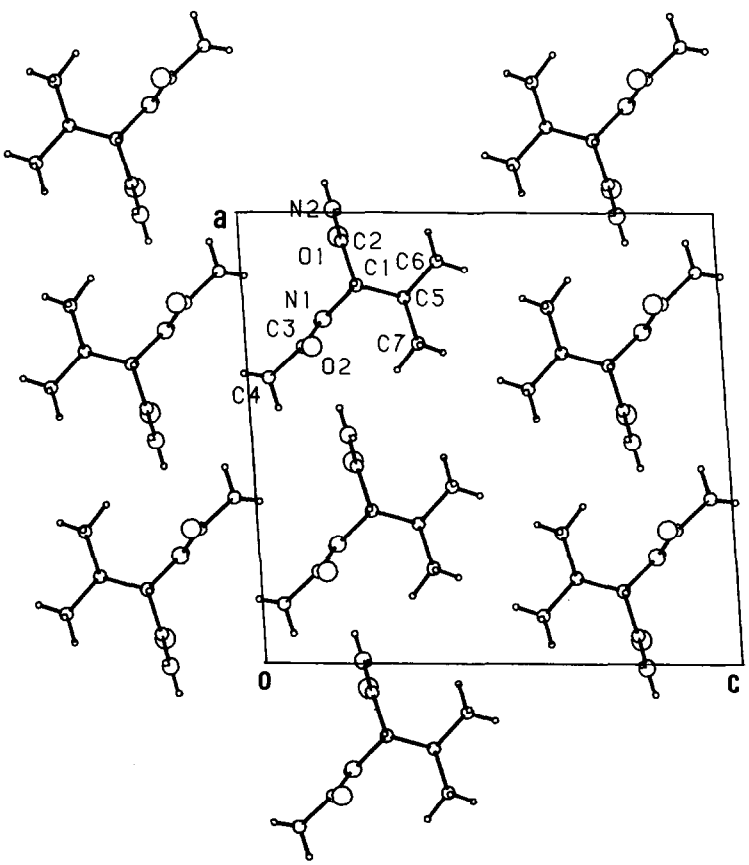

Fig. 2. Molecular assemblage of L-NAVA, viewed along the *b* direction with the labelling scheme for all non-hydrogen atoms. Two different apolar regions, parallel to the *a* axis, can be clearly observed: one at $c = 0$, the other at $c = 0.5$.

CONCLUSION

In our preceding papers [1,3], the sublimation behaviour of other amides of simple *N*-acetylated amino acids was explained by taking into account the crystal structure characteristics. In fact, in the crystals of *N*-acetyl-L-leucinamide (a mirror image of the D-enantiomers whose thermodynamic properties have been studied, see ref. 1), each molecule is involved in only four hydrogen bonds shared with the nearest neighbour molecules. The overall pattern of hydrogen bonds is bi-dimensional and the L-NALA molecules form wrinkled polar sheets, extending perpendicular to the *c* axis and making concavities similar to those of half an egg box, in which the twisted side chains are settled. In the crystals of L-NAAA, the H-bond network is also bi-dimensional, but each molecule shares six hydrogen bonds with its neighbours. In the crystals of NAGA, each molecule shares six hydrogen bonds, but in this case the molecules are interlinked by a tri-dimensional network of hydrogen bonds and the packing is much more dense than those of NAAA and NALA (1.32 g cm^{-3} versus 1.20 and 1.12 g cm^{-3} respectively). Thus, the larger number of hydrogen bonds in the crystal and the stronger intermolecular interactions due to the better packing (especially in the case of NAGA), can explain the decrease in the values of $\Delta_{sub}H_T^{\ominus}$ and $\Delta_{fus}H_T^{\ominus}$ for these three substances with increasing molecular weight. Note that, on the contrary, for both liquid alkylamides and solid amides the vaporisation or sublimation enthalpies increase, per each CH_2, by about 5 kJ mol^{-1} [23,28].

In the L-NAVA crystal, hydrogen bonds of proper length are established (Table 6), their geometry being quite similar to those observed in an earlier paper [3]. The van der Waals interactions are optimised (without forcing the conformational constraints) by forming a molecular arrangement that allows very good contacts between pairs of isopropyl side-chains and between pairs of C4 methyl groups (Fig. 2). The distances are correct for ensuring that most of the attractive forces are effective and are not so short that hydrogen repulsions become significant. The apolar layers, which are characterised by small empty domains (see Fig. 2), are much less dense than the polar layers that contain the hydrogen-bond network. This enhanced heterogeneity in the atom distribution is responsible for the relative low density of L-NAVA crystals when compared with that of L-NAAA crystals. In spite of this, the better "apolar group–apolar group" contacts may explain the greater stability of L-NAVA crystals, otherwise the density effect would overwhelm that of the increased molecular weight, as occurs for NAGA with respect to L-NAAA. It must be noted that during the solid–vapour phase transition, L-NAAA and L-NAVA molecules undergo analogous conformational rearrangements from a β-sheet form to more compact conformations, the C_5 and the equatorial C_7 [29]. In the conformational transition associated with the sublimation, the D-NALA molecule probably gains much more energy

than L-NAVA and L-NAAA. In fact it assumes folded conformations, near to those populated by L-NAAA and NAGA [29], while its crystal conformation has more energy. However the more favourable conformational rearrangement and the small number of hydrogen bonds that have to be broken, do not seem sufficient to explain the great difference between the $\Delta_{sub}H_T^{\ominus}$ values of D-NALA and L-NAVA. A contribution from the same packing characteristic of NAVA must hence be taking place, besides the contribution due to the decreased molecular weight. Work is in progress to calculate the relative energies and populations of every stable conformer in the gas phase. Even though no information on the molecular interactions and conformer distribution in the liquid state is available, analogous explanations can probably be invoked to rationalise the fusion behaviour of L-NAVA with respect to the other studied derivatives of simple amino acids.

ACKNOWLEDGEMENTS

This work was financially supported by the Consiglio Nazionale delle Ricerche (C.N.R.) and by the Ministero della Publica Istruzione.

REFERENCES

1 D. Ferro, G. Della Gatta and G. Barone, J. Therm. Anal., 34 (1988) 835.
2 D. Ferro, B. Palecz, G. Della Gatta and V. Piacente, to be published.
3 R. Puliti, C.A. Mattia, G. Barone and C. Giancola, Acta Crystallogr., C45 (1989) 1544.
4 R. Puliti, C.A. Mattia, G. Barone and C. Giancola, submitted to Acta Crystallogr.
5 G.M. Blackburn, T.H. Lilley and P.J. Milburn, J. Chem. Soc., Faraday Trans. I, 81 (1980) 915.
6 G.M. Blackburn, T.H. Lilley and P.J. Milburn, J. Chem. Soc., Faraday Trans. I, 82 (1986) 2965.
7 P.J. Cheek and T.H. Lilley, J. Chem. Soc., Faraday Trans. I, 84 (1988) 1927.
8 G. Barone, G. Castronuovo, P. Del Vecchio and V. Elia, J. Chem. Soc., Faraday Trans. I, 84 (1988) 1919.
9 G. Barone, G. Castronuovo, P. Del Vecchio and C. Giancola, J. Chem. Soc., Faraday Trans. I, 85 (1989), 2087.
10 M. Volmer, Z. Phys. Chem., Bodenstein Fastband, (1931) 863.
11 V. Piacente and G. De Maria, Ric. Sci. (Rome), 39 (1969) 549.
12 V. Piacente, P. Scardala, D. Ferro and R. Gigli, J. Chem. Eng. Data, 30 (1985) 372.
13 D. Ferro, G. Barone, G. Della Gatta and V. Piacente, J. Chem. Thermodyn., 19 (1987) 915.
14 D. Ferro and G. Della Gatta, Thermochim. Acta, 122 (1987) 189.
15 G. Della Gatta and D. Ferro, Thermochim. Acta, 122 (1987) 143.
16 P. Main, S.J. Fiske, S.E. Hull, L. Lessinger, G. Germain, J.P. Declercq and M.M. Woolfson, A System of Computer Programs for the Automatic Solution of Crystal Structures from X-ray Diffraction Data, Univ. of York, England and Louvain, Belgium, 1982.

17 D.T. Cromer and J.T. Waber, in International Tables for X-ray Crystallography, Vol. IV, Kynoch Press, Birmingham, 1974. (Present distributor D. Reidel, Dordrecht).
18 J.D. Cox and J. Pilcher, Thermochemistry of Organic and Organometallic Compounds, Academic Press, London, 1970, pp. 125–187.
19 M. Davies and G.H. Thomas, Trans. Faraday Soc., 56 (1960) 185.
20 M. Davies and B. Kybett, Trans. Faraday Soc., 61 (1965) 1608.
21 M. Davies and V.E. Malpass, J. Chem. Soc., (1961) 1048.
22 D.P. Baccanari, J.A. Novinski, Yen-Chi Pan, M.M. Yevitz and H.A. Swain, Jr., Trans. Faraday Soc., 64 (1968) 1201.
23 M. Davies, A.H. Jones and G.H. Thomas, Trans. Faraday Soc., 55 (1959) 1100.
24 E. Benedetti, in B. Weinstein (Ed.), Chemistry and Biochemistry of Aminoacids, Peptides and Proteines, Vol. VI, M. Dekker, New York, 1982, pp. 105–184.
25 S.S. Zimmerman, M.S. Pottle, G. Némethy and H.A. Scheraga, Macromolecules, 10 (1977) 1.
26 E. Benedetti, G. Morelli, G. Némethy and H.A. Scheraga, J. Peptide Protein Res., 22 (1983) 1.
27 M. Vasques, G. Némethy, and H.A. Scheraga, Macromolecules, 16 (1983) 1043.
28 G. Barone, G. Castronuovo, G. Della Gatta, V. Elia, and A. Iannone, Fluid Phase Equilibria, 21 (1985) 157.
29 P. Amodeo, V. Barone, and F. Fratenali, Thermochim. Acta, 162 (1990) 141.